Columnar mesophases of hexabenzocoronene derivatives. II. Charge carrier mobility

James Kirkpatrick,[1,2,a)] Valentina Marcon,[1] Kurt Kremer,[1] Jenny Nelson,[2] and Denis Andrienko[1,b)]
[1]*Max-Planck-Institut für Polymerforschung, Ackermannweg 10, 55128 Mainz, Germany*
[2]*Department of Physics, Imperial College London, Prince Consort Road, London SW7 2BW, United Kingdom*

(Received 15 April 2008; accepted 21 July 2008; published online 4 September 2008)

Combining atomistic molecular dynamic simulations, Marcus–Hush theory description of charge transport rates, and master equation description of charge dynamics, we correlate the temperature-driven change of the mesophase structure with the change of charge carrier mobilities in columnar phases of hexabenzocoronene derivatives. The time dependence of fluctuations in transfer integrals shows that static disorder is predominant in determining charge transport characteristics. Both site energies and transfer integrals are distributed because of disorder in the molecular arrangement. It is shown that the contributions to the site energies from polarization and electrostatic effects are of opposite sign for positive charges. We look at three mesophases of hexabenzocoronene: herringbone, discotic, and columnar disordered. All results are compared to time resolved microwave conductivity data and show excellent agreement with no fitting parameters. © *2008 American Institute of Physics*. [DOI: 10.1063/1.2969764]

I. INTRODUCTION

Discotic liquid crystalline (LC) materials are used as active elements in electronic devices due to their semiconducting properties.[1] Typical applications are field effect transistors, light emitting diodes, and solar cells.[2] In all of these applications, the rate of charge transport within organic layers plays a key role.[3]

At high temperatures, the charge carriers are localized and the transport operates by a thermally activated hopping mechanism.[4] At the microscopic level, charge transport can then be described as an electron (or hole) transfer from a charged molecule to an adjacent neutral molecule.[5] The hopping rate is given by Marcus expression

$$\omega_{ij} = \frac{J_{ij}^2}{\hbar}\sqrt{\frac{\pi}{\lambda k_B T}}\exp\left[-\frac{(\Delta G_{ij}-\lambda)^2}{4\lambda k_B T}\right], \quad (1)$$

where J_{ij} is the electronic transfer integral, λ is the molecular reorganization energy, ΔG_{ij} is the free energy difference between the initial and final states, k_B is Boltzmann's constant, and T is the temperature.

Equation (1) states that the overall rate is set by the reorganization energy, which expresses the strength of electron phonon coupling, and the intermolecular transfer integral J_{ij}, which is the matrix element of the wave functions before and after charge transfer and is hence proportional to the probability of charge tunneling between two conjugated molecules. The transfer integral can be determined from molecular orbitals. For holes it is related to the highest occupied molecular orbital (HOMO) and for electrons to the lowest unoccupied molecular orbital (LUMO). It can be computed either as the expectation value for the molecular orbitals of isolated molecules of the Fock matrix of the whole system of interacting molecules, or more simply as the overlap of the molecular orbitals of individual molecules.[6]

Simple geometrical considerations indicate that the overlap of the molecular orbitals is very sensitive to the relative position and orientation of the molecules participating in the charge transport. Hence, the charge mobility is sensitive to the local ordering of molecules, presence of structural defects, and of course to the type of the mesophase.

While the quality of the molecular arrangement (defect-free structures) is determined largely by processing, the type of the mesophase and local ordering depend on the chemical structure of a particular compound as well as intensive thermodynamic properties, such as temperature and pressure. Typical discotics consist of a flat aromatic core with aliphatic chains attached at the edges. The overlap of π-orbitals of adjacent cores provides means for charge migration, while the side chains attached to the core ensure solubility (i.e., good processability of materials) as well as capacity for self-organization. Hence, the ability to conduct charge carriers can be tuned either via synthesis, by changing the shape and size of the conjugated core or the side chains, or, alternatively, by inducing a mesophase favorable to charge transport.

In the first part of this contribution, we have studied phase transitions in hexabenzocoronenes (HBCs) with three types of side chains: alkyl chains of length 12 C_{12}; branched side chains, C_{10-6}; and dodecylphenyl-substituted PhC_{12} side chains, the molecular structures of which are shown in Fig. 1. These systems posses qualitatively different mesophase ordering[7,8] and, as a result, quantitatively different charge carrier mobilities.[9–11] We have shown that atomistic simulations are capable of reproducing phase transitions in these

a)Electronic mail: james.kirkpatrick@imperial.ac.uk.
b)Electronic mail: denis.andrienko@mpip-mainz.mpg.de.

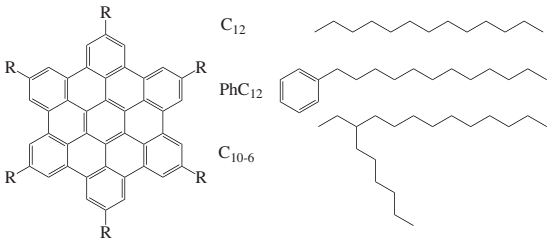

FIG. 1. Studied derivatives of hexabenzocoronene.

systems.[7,12] Summarizing the results from the first part of this contribution,[12] C_{12} shows a clear phase transition from a herringbone to a discotic mesophase at 380 K. For PhC_{12}, the herringbone phase is unstable at room temperature, and the system tends to stay in the discotic phase. C_{10-6} shows a transition from a herringbone to a columnar disordered phase at 320 K. It was also possible to study the change in local order of the morphologies within each phase. In this study, these data will be used to determine whether the simulated morphology changes with mesophase symmetry are consistent with the temperature dependence of experimental mobility. To do this, we employ the methodology developed in our previous works,[9–11] where we have shown that the charge transport in columnar phases of discotic LCs can be described at a quantitative level. The prescribed methodology deduces the local morphologies from molecular dynamics (MD) simulations, obtains the charge transport rates from Marcus–Hush formalism, and mimics the time-of-flight experiments using kinetic Monte Carlo approach.

Here we extend this method to study the *temperature* dependence of charge mobility of HBCs furnished with different side chains. We first perform an analysis of the variation in charge transport parameters (site energies and transfer integrals) as a function of temperature. We then analyze the time scale for fluctuations of the transfer integrals and argue that HBCs are not treated well either by a Haken–Strobl–Reineke model[13] (where random fast fluctuations are considered, but slow variations are ignored) nor by the Troisi model[14] (where variations in transfer integrals are mediated by classical, intermolecular vibrations).

In particular, we seek to explain two experimental features of the charge transport in these materials; the sudden decrease of mobility in the liquid crystalline phase with respect to the crystalline phase and the weak dependence of mobility on temperature within each phase. We show that the sudden decrease in mobility upon phase change is due to the changes in rotational register of neighboring molecules. The weak dependence of mobility on temperature is found to be consistent with a small polaron, temperature activated model for charge transport.

II. COMPUTATIONAL METHODS

Transfer integrals are calculated using an approximation of Zerner's semiempirical intermediate neglect of differential overlap (INDO).[6] Only the closest intracolumnar neighbors are considered, leading to two neighbors per molecule. Since the highest degenerate and lowest unoccupied molecular orbitals (HOMO and LUMO) of HBC are doubly occupied, it is necessary to compute all four possible combinations of transfer integrals and take the root mean square average,[15]

$$J_{ij} = \tfrac{1}{2}(J^2_{\mathrm{HOMO}_i,\mathrm{HOMO}_j} + J^2_{\mathrm{HOMO}_i,\mathrm{HOMO-1}_+} + J^2_{\mathrm{HOMO-1}_i,\mathrm{HOMO}_j} + J^2_{\mathrm{HOMO-1}_i,\mathrm{HOMO-1}_j})^{1/2}. \quad (2)$$

The internal reorganization energy λ (for holes) was calculated as[16]

$$\lambda = E^n_+ - E^n_0 + E^c_0 - E^c_+, \quad (3)$$

where E^n_0 and E^c_+ represent the energies of the neutral and cation species, respectively, in their lowest energy geometries, while E^c_0 and E^n_+ represent the energies of the neutral and cation species with the geometries of the cation and neutral species, respectively (superscript refers to the geometry and subscript to the charge). A value of 0.1 eV was obtained using the B3LYP functional and 6–311g(d,p) basis set.

Site energy disorder exists because the electric field and polarizability of molecules is nonisotropic, and hence disorder in molecular orientation or position is sufficient to lead to a different energetic landscape at different points along the column. We assume that there are two main contributions to site energy differences ΔG_{ij}: an electrostatic contribution and a contribution due to polarization effects. The importance of electrostatic contribution has long been recognized for charge transport in polar molecules dispersed in an inert matrix[17] and is also one of the mechanisms believed to be responsible for long range correlations in conjugated polymers.[18]

In the case of HBC, we want to be able to model the effect of both the local dipole moments between aromatic carbons and hydrogen atoms and the quadrupole moment due to the negative π electrons delocalized below and above the molecular plane. Of these two electric moments, the first can be easily described by point charges located at each atomic position, but the second cannot. In order to represent quadrupoles, we placed a layer of point charges above and below the carbons in the conjugated core. These ghost charges are located at 0.47 Å from the carbons, in accordance with previous studies by Hunter[19] on the influence of quadruples on π stacking. Density functional theory calculations [B3LYP, 6–311g(d,p)] of a neutral and charged molecule were then performed, and electrostatic charges were fitted, using the CHELPG method,[20] to both the ghost atoms and "normal" atoms in the HBC core. From the MD simulation, we know the position and orientation of all molecules in the column. If the electrostatic energy between two molecules is written as $V(\alpha i, \beta j)$, where i and j are molecular indices and α and β describe whether the EPS charges on molecule correspond to a charged (α=+) or neutral (α=0) molecule, it is possible to describe the energy V_i corresponding to having a charge on molecule i as

$$V_i = \sum_{j \neq i} V(+i, 0j) - V(0i, 0j), \quad (4)$$

where the energy V_i is then given with respect to the energy of the neutral system. Since the side chains are neutral, we only consider isolated columns when calculating site energy differences.

Electrostatic interaction are long ranged, and in order to extrapolate the energy differences to the infinite system, the sum in Eq. (4) can be evaluated for the simulation box with the charged molecule in the middle padded by extra (neutral) boxes. However, since in our system the lowest order molecular multipole is the quadrupole, expression (4) converges rapidly with the number of padding cells. In fact, the site energy differences calculated using a single simulation box are the similar to those calculated by padding the box with extra boxes to within 6%.

Polarizability has also been shown to be important in stabilizing the energies of neutral and charged aromatic crystals.[21] In order to calculate its contribution to the site energy differences, it is sufficient to know the difference in energy for a charged crystal with the charge localized in one particular place and one with the charge localized elsewhere. To model this effect, we use a model of polarizable force field[22,23] and include point polarizable dipoles on each carbon atom of the HBC core. Following Ref. 23, we take a polarizability of 0.7 $Å^3$ with no cutoff radius for aromatic carbons. The polarization energy of the system then has three contributions: from the external field (in our case caused by the point charges from EPS fitting), from the interaction of the induced dipoles with each other, and from the self-energy of the dipoles. Equations for the corresponding polarizabilities can be either solved self-consistently or via matrix inversion. Since we tend to work with systems with less than 2000 polarizable sites, we find matrix inversion more convenient computationally.

A. Charge transport mobilities

In our previous study, we used kinetic Monte Carlo methods to determine charge transport characteristics. Since our systems have relatively low disorder, the steady state mobility is similar to the transient mobility, and we can use the master equation method[24]

$$\frac{\partial P_i}{\partial t} = \sum_j [\omega_{ij} P_j (1 - P_i) - \omega_{ji} P_i (1 - P_j)], \tag{5}$$

where P_i is the probability of a charge to be on a site i, ω_{ij} is the hopping rate from site j to site i, and t is time. Since our systems are very ordered and since we are interested in low charge density, the nonlinear master Eq. (5) yields very similar results to the corresponding linear equation,

$$\frac{\partial P_i}{\partial t} = \sum_j [\omega_{ij} P_j - \omega_{ji} P_i]. \tag{6}$$

We solve this equation by setting the left hand side to zero and seeking roots to the problem via standard linear techniques.

The charge mobility μ is then determined from the charge velocity

$$\boldsymbol{v} = \sum_{ij} \omega_{ji} P_i (\boldsymbol{r}_j - \boldsymbol{r}_i),$$

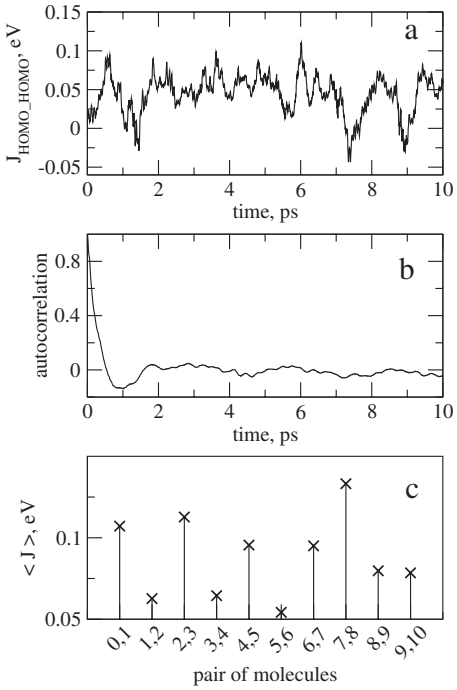

FIG. 2. (a) Variation of the transfer integral $J_{\text{HOMO-HOMO}}$ between a pair of molecules at 300 K. (b) Autocorrelation function of fluctuations in transfer integrals averaged over all pairs and all four integrals. (c) Average over 20 ps of the effective transfer integral for all pairs of molecules.

$$\boldsymbol{v} = \mu \boldsymbol{F}, \tag{7}$$

where $\boldsymbol{r}_i$ is the coordinate of the site i and $\boldsymbol{F}$ is the applied electric field. The linearized master equation approach was compared to the kinetic Monte Carlo method used in our previous study and yielded similar results at a fraction of the computational cost.

III. RESULTS AND DISCUSSION

A. Fluctuations in transfer integrals

As in previous work,[9] we shall base our mobility simulations on snapshots from MD trajectories. In order to justify this choice, we have looked at fluctuations in transfer integrals from very short trajectories of 20 ps with a time resolution of 2 fs. A time scale of 20 ps is comparable to the characteristic time for electronic hopping (time between two consecutive hops). In a system with reorganization energy $\lambda = 0.13$ eV and a transfer integral $J = 50$ meV, the inverse of the rate predicted by Eq. (1) is 1.6 ps. In particular, we want to compare our approximation that charge transport occurs on a frozen lattice with two models: the Haken–Strobl–Reineke model,[25] where fluctuations are very fast but no static disorder is allowed, and the Troisi model,[14] where variation in the transfer integral are mediated by classical, intermolecular phonons.

The temporal variation of the transfer integral $J_{\text{HOMO-HOMO}}$ between a pair of molecules is shown in Fig. 2(a). One can see that the transfer integral fluctuates significantly already even on a subpicosecond time scale. To characterize the fluctuation spectrum, we calculate the autocorrelation function of the transfer integral for each pair of molecules and for all four hole transfer integrals. We then

average the autocorrelation functions over all pairs and all hole transfer integrals. The result is shown in Fig. 2(b). One can see that the autocorrelation function decays very rapidly with time. This situation is in sharp contrast with that present in molecular crystals.[14] In that case, the transfer integrals do not decorrelate from each other over the time scale of the MD simulations. The oscillations in transfer integrals are slow and their power spectrum reveals that they can be associated to specific phonon modes. In our case, the autocorrelation function decays rapidly and the initial part of it cannot be fitted with a single exponential, which is a consequence of not having a single relaxation time for a molecular motion (e.g., azimuthal and polar molecular rotations have different relaxation times).

Given this fast decay in the autocorrelation function of the transfer integral, the approximation of the Haken–Strobl–Reineke model used in Ref. 25 seems reasonable. The key assumption in this model is that the autocorrelation function of the transfer integral can be approximated with a delta function, in other words fluctuations in transfer integrals are much faster than the time scale for electronic tunnelling $(J/\hbar)$, which, taking 50 meV as a transfer integral, has a value of 80 fs in this system. The issue with our systems is that although these almost instantaneous variations in transfer integrals do indeed occur, each pair of molecules in the system is *not* equivalent. That is to say, the system accommodates both very fast fluctuations and very slow fluctuations in transfer integral. This is illustrated in Fig. 2(c), where we show 20 ps averages of the transfer integral for all neighbors in a single column. The variation of these values occurs on a much longer time scale, of the order of nano- and microseconds, due to rotational diffusion of molecules and fluctuations of macroscopic degrees of freedom, such as density and order parameter.[26]

In HBC, charge transport is one dimensional, therefore the smallest transfer integrals of the distribution dominate the rate[9] of charge transfer. In the context of nonadiabatic transport, the transfer integrals should be averaged over the time scale of charge transfer,[27] with a correction term added to allow for excitations from the vibrational modes causing the transfer integral to fluctuate. Variations in transfer integrals depend on fast and slow fluctuations. If we averaged out the fast fluctuations, the distribution of integrals would become somewhat narrower and we would be liable to somewhat overestimate the charge transfer rates. Doing this leads only to a small overestimate of the mobility (of 25% in the case of positive charge transport at a temperature of 420 K). We only include the effect of slow (static on the time scale of electron transfer) variations in transfer integral by calculating mobility for many uncorrelated snapshots and averaging the mobilities, rather than accurately describing the fast fluctuations.

B. Distribution of transfer integrals

Figure 3(a) shows two representative histograms of the $\log_{10}(J_{ij})$ squared made for a long (40 ns) run for the dovetail (C_{10-6}) derivative at two temperatures, above and below the phase transition 240 and 480 K. At low temperatures, in a herringbone mesophase, the distribution is practically Gaussian with a well defined mean and standard deviation. Upon increasing the temperature, the distribution broadens and, above the phase transition to the liquid crystalline mesophase, develops a long tail extending into the region of small transfer integrals (note the logarithmic scale on the y axis of the plot). The mean and the standard deviation of the distribution of the transfer integrals are the two key parameters entering many phenomenological models of charge transport [e.g., Gaussian disorder model (GDM)]. We will now discuss the variation of these parameters with temperature for the three derivatives separately.

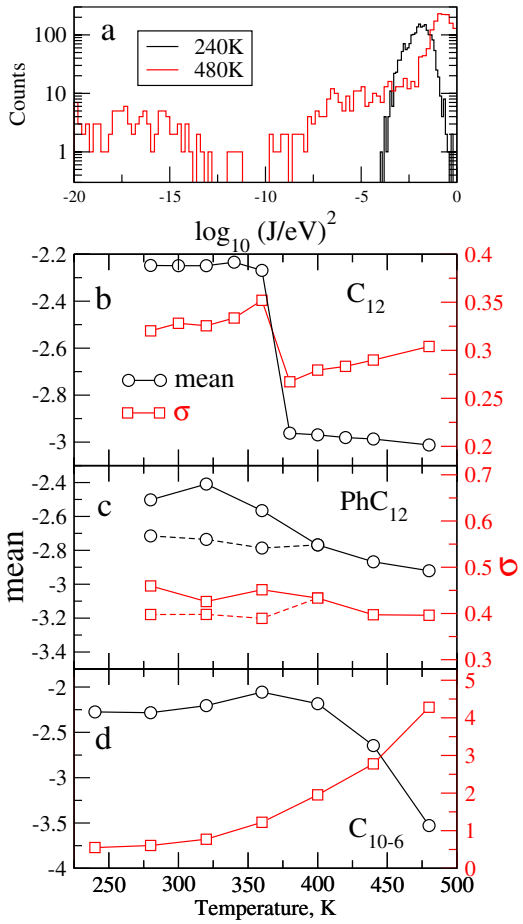

FIG. 3. (Color online) (a) Distribution of $\log J^2$ for the dovetail (C_{10-6}) derivative at 240 and 480 K. Note the logarithmic scale on the y axis. Average and standard deviation of the distribution of $\log J^2$ for (b) C_{12}, (c) PhC_{12}, and (d) C_{10-6} derivatives. Dashed lines indicate "annealed" samples.

Figures 3(b)–3(d) show the variation with temperature of the standard deviation and mean in distribution of $\log_{10}(J_{ij})$ for the three derivatives considered. For the derivative with linear aliphatic side chains (C_{12}), the most obvious feature is the dramatic decrease in transfer integral upon phase transition from a herringbone to a discotic structure at 360 K. $|J_{ij}|^2$ falls by almost a decade, suggesting that the hole mobility will similarly be affected. The width of the distribution in contrast is left relatively unchanged. This sharp fall in transfer integral can readily be understood in terms of variations of molecular overlap. In the low temperature herringbone phase, the molecules are shifted with respect to each other but are not rotated with respect to each other. In the high

temperature discotic liquid crystalline phase, molecules are placed directly on top of each other and rotated by approximately 30°. Since at 30° one has a minimum in the molecular overlap, the transfer integral in the discotic phase tend to be rather small. One should also note that in both phases, the width of the distribution of the logarithm of the transfer integrals is rather large, at around a third of a decade and that widths tend to be slightly larger for the herringbone phase, which is in agreement with the fact that the lateral twist angle has a wider distribution for the herringbone than for the hexagonal phase, as it can be seen from Fig. 10 in Paper I.[12] As noted in our previous work, since transport in HBC is one dimensional, it is not so much the average transfer integrals that dominates the mobility of a column, but rather the tail of low transfer integrals.

In the PhC_{12} derivative, the mean and standard deviation of the transfer integral do not vary abruptly with temperature. This is consistent with the fact that a phase transition is not observed. It is also interesting to note that the absolute mean and width of the distribution of $\log_{10}(J_{ij})$ are rather similar to those obtained in the discotic phase.

Note that at low temperatures, the systems were prepared in a rectangular lattice and the time scale for destroying this order was longer than the longest MD time scale accessible (MD is limited to equilibration times of about 100 ns). To allow better equilibration, we first annealed the systems at 500 K and then performed MD at 280, 320, and 360 K starting from the end configurations obtained from high temperature simulations. The distributions in transfer integral obtained are shown in Figs. 3(c) as a dotted line. It can be seen that results obtained from such "annealing" procedure produce more evenly distributions across columns.

In the case of the dovetail derivative, shown in the bottom of Fig. 3, the mean falls sharply with temperature after a slight increase and the standard deviation increases steadily. Figure 3(a) shows the distribution of $\log_{10} J_{ij}^2$ at different temperature. As the temperature is increased, the median of transfer integrals squared is increased; however, a large tail of low transfer integrals appears. In other words, at low temperatures, the system is in a crystalline state with a typical Gaussian distribution of logarithm of transfer integrals. As the temperature increases, the system enters what Pisula *et al.* call a disordered columnar phase.[28] In this phase, there is an overall columnar order, but each molecule has no ordering with respect to its neighbors. As our previous contribution shows, the MD simulations suggest that several molecules tend to form very well packed and well ordered clusters, which are themselves disorganized in the column. In such an arrangement, the mode of the transfer integral increases because the short segments of column, which are well packed, are better packed than in the crystalline phase. However a large tail of transfer integral appears corresponding to pairs of molecules on different well packed fragments of columns.

To conclude this part, we have seen how in all three materials the width and mean of the distribution of the transfer integrals is controlled by the phase that the material is in. Discotic phases have smaller mean transfer integrals, but seem slightly more ordered than herringbone phases. The disordered columnar discotic phase of the dovetail derivative is intriguing. On one side it shows the best coupling between nearest neighbors, but on the other side it has the longest tail of low lying transfer integrals. It also appears that the dovetail derivative is significantly more disordered, with less homogeneity between the columns, than any other derivative studied.

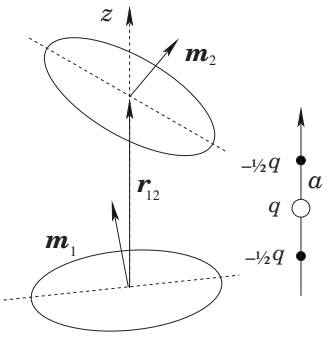

FIG. 4. Schematic figure of two molecules defined as point sources of electric field (left). Schematic description of the charge distribution of a linear quadrupole.

C. Energetic disorder

We now look at the role of energetic disorder in our systems. In order to better understand the relative importance of electrostatic and polarization components, we consider a simple system consisting of only two molecules. This is for illustrative purposes in order to give a feeling for how electrostatic and inductive contributions to energetic disorder occur. Each molecule is separated from the other by a center to center distance r_{12}, and its orientation is defined by $\boldsymbol{m}^{(i)}$, $i=1,2$, which is perpendicular to the molecular plane, as shown in Fig. 4. This model is supposed to be a representation of two HBC molecules: along the $\boldsymbol{m}$ axis the π electrons form a linear quadrupole, which is the lowest order multipole of a neutral HBC; also along this axis the molecule is far less polarizable than in the molecular plane.

In the case where only electrostatic contributions are considered, $\boldsymbol{m}$ is the principle axis of a linear quadrupole and the difference in site energy is simply the energy difference between the states with the charge being on the molecule (1) and it being on the molecule (2). This can be readily evaluated from the interaction energy of a point charge e on the molecule (1) with a quadrupole $Q_{ij}^{(1)}$ on a molecule (2),

$$U^{(1)}(\boldsymbol{r}_{12}) = \frac{1}{4\pi\epsilon_0}\frac{eQ_{ij}^{(1)}n_i n_j}{2r_{12}^3}, \tag{8}$$

where $\boldsymbol{n}$ is a unit vector along $\boldsymbol{r}_{12}$.

Rewriting Eq. (8) in a reference frame with $\boldsymbol{r}_{12}$ along the z axis ($\boldsymbol{n}=\boldsymbol{e}_z$), we obtain

$$U(\boldsymbol{r}_{12}) = \frac{1}{4\pi\epsilon_0}\frac{eQ_{zz}^{(1)}}{2r_{12}^3}, \tag{9}$$

where Q_{zz} is in the coordinate system with $\boldsymbol{n}$ along $\boldsymbol{e}_z$.

$Q_{ij}^{(1)}$ is a symmetric traceless tensor; hence it can be written as

$$Q_{ij}^{(1)} = \frac{Q}{2}(3m_i^{(1)}m_j^{(1)} - \delta_{ij}). \tag{10}$$

The zz component of this tensor then reads

$$Q_{zz}^{(1)} = \frac{Q}{2}[3(m_z^{(1)})^2 - 1] = \frac{Q}{2}[3(\boldsymbol{m}^{(1)} \cdot \boldsymbol{n})^2 - 1]. \tag{11}$$

For our systems, where a positive charge is sandwiched by negative charges, Q has a negative value.

Substituting Eq. (11) into Eq. (8) and taking the energy difference between the charge being on the molecule (1) and it being on the molecule (2), we obtain the difference in site energy

$$\Delta G_{\text{est}} = U^{(1)} - U^{(2)} = \frac{3eQ}{16\pi\epsilon_0 r_{12}^3}(\gamma^{(1)} - \gamma^{(2)}), \tag{12}$$

where $\gamma^{(i)} = (\boldsymbol{n} \cdot \boldsymbol{m}^{(i)})^2$.

This formula tells us that in order to have nonzero site energy difference, it is necessary that the molecules do not have the same projection of their normal vectors on the intramolecular vector $\boldsymbol{r}_{12}$, i.e., they should be tilted with respect to each other. This means that in an ideal herringbone or columnar mesophase, where all molecules are parallel to each other, the electrostatic site energy difference is zero. Only out-of-plane molecular fluctuations will lead to the energetic disorder due to electrostatic contribution.

Let us now consider the case where only polarization is considered. We consider two polarizable dipoles with the axially symmetric polarizability tensor $\hat{\boldsymbol{\alpha}}$. The complete problem, involving polarization of both dipoles, can be solved using the approach of Ref. 23. If we ignore effects quadratic in polarizability, the electrostatic energy of a system with a charge e at a molecule (1) and induced dipole $\boldsymbol{\mu}_2$ at (2) reads

$$U^{(1)} = \boldsymbol{\mu}_2 \boldsymbol{E}_2 = \left(\frac{e}{4\pi\epsilon_0 r_{12}^2}\right)^2 (\hat{\boldsymbol{\alpha}} \cdot \boldsymbol{e}_z) \cdot \boldsymbol{e}_z. \tag{13}$$

Note that this expression is again written in the coordinate system with $\boldsymbol{r}_{12}$ parallel to the z axis. Introducing two vectors orthogonal to each other and to $\boldsymbol{m}^{(2)}$, $\boldsymbol{k}^{(2)} = \boldsymbol{n} \times \boldsymbol{m}^{(2)}$, $\boldsymbol{l}^{(2)} = \boldsymbol{k} \times \boldsymbol{m}^{(2)}$, we can rewrite the axially symmetric polarizability tensor $\hat{\boldsymbol{\alpha}}$ as

$$\hat{\boldsymbol{\alpha}}^{(2)} = \alpha_{\parallel}(\boldsymbol{k}^{(2)} \otimes \boldsymbol{k}^{(2)} + \boldsymbol{l}^{(2)} \otimes \boldsymbol{l}^{(2)}) + \alpha_{\perp}\boldsymbol{m}^{(2)} \otimes \boldsymbol{m}^{(2)}. \tag{14}$$

Substituting this back to Eq. (13), we obtain

$$U^{(1)} = \left(\frac{e}{4\pi\epsilon_0 r_{12}^2}\right)^2 [\alpha_{\parallel}(\gamma^{(1)} - 1)^2 + \alpha_{\perp}\gamma^{(1)}], \tag{15}$$

where as before, $\gamma^{(i)} = (\boldsymbol{n} \cdot \boldsymbol{m}^{(i)})^2$.

Taking into account that the HBC molecule is far less polarizable along the normal axis $\boldsymbol{m}$ than in the molecular plane ($\alpha_{\parallel} \gg \alpha_{\perp}$), we obtain the site energy difference

$$\Delta G_{\text{pol}} = \left(\frac{e}{4\pi\epsilon_0 r_{12}^2}\right)^2 \alpha_{\parallel}\{(1 - \gamma^{(1)})^2 - (1 - \gamma^{(2)})^2\}. \tag{16}$$

Comparing Eqs. (12) and (16) and remembering that Q is negative, one can see that for positive values of e and $\alpha_{\perp}$ polarization tends to reduce the energetic disorder caused by electrostatics. It should also be noted that the electrostatic contributions fall more slowly with distance. It is interesting to note that this analysis is rather general to π stacked molecules and that it suggests that disorder is intrinsically greater for negative charges than for positive charges in those materials.

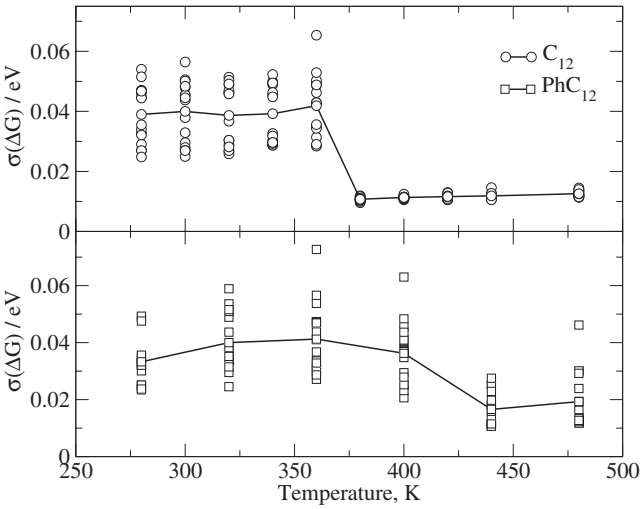

FIG. 5. Standard deviation σ of the distribution of site energy difference for C_{12} (circles) and PhC_{12} (squares).

We now come back to the analysis of the MD trajectories. Figure 5 shows the dependence of energetic disorder on temperature for the C_{12} and the PhC_{12} derivatives. We plot the standard deviation of the distribution of site energy differences between nearest neighbors, which we will refer to as energetic disorder, in accordance with the GDM. One should note, however, that in the GDM, energetic disorder refers to the width in site energies, whereas in our case it corresponds to the width in the *difference* in site energies. The site energy differences analyzed are the sum of the electrostatic and polarization components.

We find that the polarization component generally constitutes the smaller part of the site energy disorder in our computation and, in accordance to our approximate arguments above, tends to lower the magnitude of the energetic disorder. For example, the average value of the energetic disorder for C_{12} at 320 K is 54 meV if polarization is ignored and 28 meV if it is included.

Analyzing Fig. 5, one can notice two things. In the C_{12} derivative, significant energetic disorder is present only in the herringbone phase, and in the PhC_{12} derivative, energetic disorder is far less temperature dependent and is large compared to the discotic phase of C_{12}. The larger energetic disorder in the PhC_{12} derivative can be explained by looking at the distribution functions for the intermolecular distances.[12] These show that this derivative is more disordered than the C_{12} derivative. The origin of mesophase dependence of energetic disorder in the C_{12} derivative is not obvious. It is possible that just as wave function overlap is stronger when adjacent molecules are in rotational register, electrostatic interactions are also stronger. Due to computational constraints, energetic disorder for the dovetail derivative was not computed.

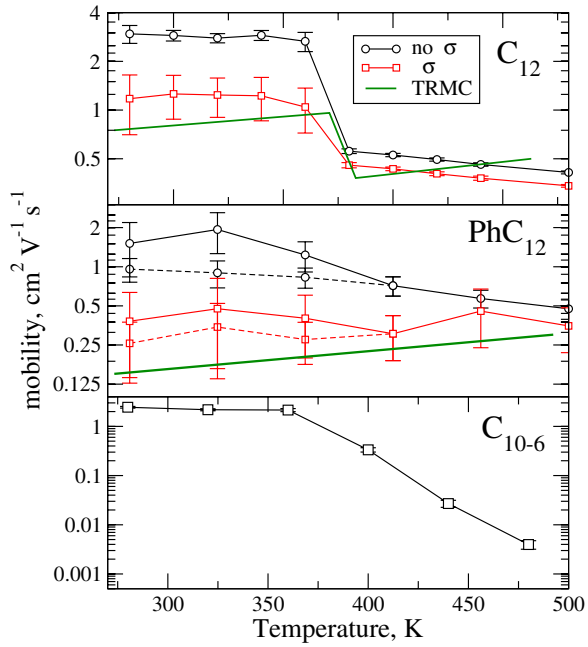

FIG. 6. (Color online) Hole mobility including (circles) and excluding (squares) the effect of energetic disorder compared to the experimental PR-TRMC data (solid line) for three derivatives C_{12}, PhC_{12} and C_{10-6}. In the case of C_{10-6} the experimental TRMC mobility (Ref. 28) in the crystalline plastic phase is 0.7 $cm^2\ V^{-1}\ s^{-1}$ and in the columnar disordered phase is 0.08 $cm^2\ V^{-1}\ s^{-1}$. Note logarithmic scale on the y axis.

D. Mobility simulation

Figure 6 shows the temperature dependence of hole mobility, obtained including and excluding energetic disorder for the C_{12} and PhC_{12} in comparison to the data from PR-TRMC.[29] It should be noted that in all three cases, we overestimate the mobility, especially if energetic disorder is not included. Inclusion of energetic disorder makes the comparison with experiment better, as it reduces mobility. In the case of C_{12} derivative, energetic disorder also makes the ratio of the mobility in the columnar and crystalline phase much closer to experiment. In the case of PhC_{12}, energetic disorder (and to some extent the choice of starting conditions for the low temperature runs) makes the temperature dependence more positive and more similar to experiment. In other words, energetic disorder does not simply renormalize the mobility, but helps in reproducing the correct functional temperature dependence.

The phase behavior of the dovetail derivative is rather complex, with the crystalline phase turning to columnar upon heating beyond 310 K, whereas the columnar disordered phase is stable upon decreasing the temperature. As discussed in the first part of this paper,[12] we underestimate the phase transition temperature for the crystalline to columnar disordered phases. Having acknowledged that we do observe two regimes of mobility, at low temperature in the crystalline phase, we compute a large mobility, 2.2 $cm^2\ V^{-1}\ s^{-1}$, and as we go into a hexagonal columnar phase, the mobility falls exponentially with temperature due to the appearance and lengthening of a tail of low lying transfer integrals. Experimentally measured by PR-TRMC mobility is, in fact, the sum of electron and hole mobilities. Our previous study,[9] however, shows that electron mobility is always about 20% of the hole mobility. Including it would constitute only a small systematic increase of the total value.

Figure 6 shows that sometimes our simulated mobilities are slightly negatively temperature dependent. At first sight this seems counterintuitive as polaron hops faster at higher temperature due to increase of hoping rates with temperature. To explain this, let us consider a simple model system. We assume that all transfer integrals are the equal and all molecules are at the same distance d from each other. We also neglect energetic disorder; in this case the only source of site energy differences is the applied field F.

In the limit of small fields Marcus rates along and against the field (forward and backward rates ω_f, ω_b) can be written as

$$\omega_{f,b} \sim \frac{1}{\sqrt{\lambda kT}} \exp\left(-\frac{\lambda}{4k_BT}\right)\exp\left(\pm\frac{Fd}{2k_BT}\right). \tag{17}$$

The ratio of these rates ω_b/ω_f sets the ratio of the number of backward hops N_b to forward hops N_f. Noting that the total distance traveled by a charge along the field is $D = d(N_f - N_b)$ and the total time it takes for such hops is $\tau = N_f/\omega_f + N_b/\omega_b$, we can write charge velocity as

$$v = D/\tau \propto \frac{d\omega_f}{2}\left(1 - \frac{N_b}{N_f}\right), \tag{18}$$

where $f = Fd/k_BT$. Taking into account that, for small $f = Fd/k_bT$, $\exp f \sim 1 + f$ and dropping all the temperature independent prefactors we obtain the mobility

$$\mu = v/F \propto (k_BT)^{-3/2} \exp\left(-\frac{\lambda}{4k_BT}\right). \tag{19}$$

Taking the derivative of this quantity with respect to, T we obtain

$$\frac{d\mu}{dt} \propto (k_BT)^{-5/2} \exp\left(-\frac{\lambda}{4k_BT}\right)\left(\frac{\lambda}{4k_BT} - \frac{3}{2}\right). \tag{20}$$

In other words the mobility will be negatively temperature dependent, so long as $\lambda < 6k_BT$. This is exactly the regime we find ourselves in ($\lambda = 0.1$ eV) so therefore it should come as no surprise that our mobilities are slightly negatively field dependent. Such competition between nondirectional and directional hopping has also been theoretically shown to occur in resonant tunnelling hopping in quantum dots.[30]

At this point we can review our ansatz that charge transport occurs by hopping in HBC. It is certainly hard to justify this choice uniquely on the basis that the transfer integrals are small compared to the reorganization energy, as this is not always the case. The distributions in transfer integrals are suitably wide, and adiabatic transport is indeed possible. However, we point out that treating transport as bandlike is unlikely to yield lower values of the mobility, or indeed more positively field dependent ones. We suggest that it is highly likely that both types of transport simultaneously occur and that the quantitatively good agreement between our simulations and the experimental data are due to the fact that transport is one dimensional and therefore the slowest rates determine the mobility. Our simulation result in very good

agreement with experiment, with two minor deviations. We slightly overestimate mobilities and we predict a slightly more negative temperature dependence. The slight overestimation of mobilities might be due to either a systematic overestimate of transfer integrals because of the use of the INDO formalism, or possibly to the fact that our systems are too small to include enough disorder. The fact that our simulations predict a temperature dependence slightly more negative than that actually observed, suggests either that we are ignoring some sources of energetic disorder such as chemical defects or that the experimental mobility does not reflect the real temperature dependence of the material. This is not entirely unlikely, as the yield of charges scavenged separately by neighboring columns is assumed to be independent of temperature in the PR-TRMC experiments, though it is possible that it increases slightly with temperature leading to an apparently more positively temperature dependent mobility than in reality.[31]

IV. CONCLUSIONS

The main result from this study is that mobility is determined, within the same class of materials, by mesophase alone. In the columnar and crystalline mesophases, all three materials are indeed very similar. Discotic phases have smaller mobilities than crystalline ones. The disordered crystalline phase shows the worst mobility. We have shown that these changes can be quantitatively explained in terms of distributions of transfer integrals and of energetic disorder. We have shown that qualitative and quantitative reproduction of the PR-TRMC data is possible using charge hopping rates from Marcus theory. We have shown that the fast fluctuations of transfer integrals have a small effect on the predicted mobility, that site energy disorder as computed from electrostatic and polarization contributions makes the agreement with experimental data better. Finally we have argued that a weak, or even negative, temperature dependence of mobility is not in contradiction with polaron hopping.

ACKNOWLEDGMENTS

This work was partially supported by DFG via International Research Training Group between Germany and Korea and grant "Adaptive multiscae simulation for organic electronics." V.M. acknowledges Alexander von Humboldt foundation. J.K. acknowledges the EPSRC. V.M., K.K. and D.A. acknowledge the Multiscale Materials Modeling Initiative of the Max Planck Society. Discussions with A. Troisi, K. Müllen, H. W. Spiess, W. Pisula, R. Graf, and M. Mondeshki are gratefully acknowledged.

[1] F. J. M. Hoeben, P. Jonkheijm, E. W. Meijer, and A. P. H. J. Schenning, Chem. Rev. (Washington, D.C.) **105**, 1491 (2005).
[2] S. Chandrasekhar and S. K. Prasad, Contemp. Phys. **40**, 237 (1999).
[3] F. C. Grozema and L. D. A. Siebbeles, Int. Rev. Phys. Chem. **27**, 87 (2008).
[4] R. A. Marcus, Rev. Mod. Phys. **65**, 599 (1993).
[5] V. Lemaur, D. A. Da Silva Filho, V. Coropceanu, M. Lehmann, Y. Geerts, J. Piris, M. G. Debije, A. M. Van de Craats, K. Senthilkumar, L. D. A. Siebbeles, J. M. Warman, J. L. Bredas, and J. Cornil, J. Am. Chem. Soc. **126**, 3271 (2004).
[6] J. Kirkpatrick, Int. J. Quantum Chem. **108**, 51 (2008).
[7] D. Andrienko, V. Marcon, and K. Kremer, J. Chem. Phys. **125**, 124902 (2006).
[8] V. Marcon, J. Kirkpatrick, W. Pisula, and D. Andrienko, Phys. Status Solidi B **245**, 820 (2008).
[9] J. Kirkpatrick, V. Marcon, J. Nelson, K. Kremer, and D. Andrienko, Phys. Rev. Lett. **98**, 227402 (2007).
[10] J. Kirkpatrick, V. Marcon, J. Nelson, and D. Andrienko, Phys. Status Solidi B **245**, 835 (2008).
[11] D. Andrienko, J. Kirkpatrick, V. Marcon, J. Nelson, and K. Kremer, Phys. Status Solidi B **245**, 830 (2008).
[12] V. Marcon, T. Vehoff, J. Kirkpatrick, C. Jeong, D. Y. Yoon, K. Kremer, and D. Andrienko, J. Chem. Phys. **129**, 094505 (2008).
[13] M. Palenberg, R. Silbey, M. Malagoli, and J. Bredas, J. Chem. Phys. **112**, 1541 (2000).
[14] A. Troisi and G. Orlandi, J. Phys. Chem. **110**, 4065 (2006).
[15] M. Newton, Chem. Rev. (Washington, D.C.) **91**, 767 (1991).
[16] G. R. Hutchison, M. A. Ratner, and T. J. Marks, J. Am. Chem. Soc. **127**, 2339 (2005).
[17] P. Borsenberger, L. Pautmeier, and H. Bassler, J. Chem. Phys. **94**, 5447 (1991).
[18] S. V. Novikov and A. V. Vannikov, J. Phys. Chem. **99**, 14573 (1995).
[19] C. A. Hunter and J. K. M. Sanders, J. Am. Chem. Soc. **112**, 5525 (1990).
[20] C. Breneman and K. Wiberg, J. Comput. Chem. **11**, 361 (1990).
[21] E. V. Tsiper and Z. Soos, Phys. Rev. B **68**, 085301 (2003).
[22] P. Ahlström, A. Wallqvist, S. Engström, and B. Jönsson, Mol. Phys. **68**, 563 (1989).
[23] H. A. Stern, G. A. Kamisnki, J. L. Banks, R. Zhou, B. J. Berne, and R. A. Friesner, J. Phys. Chem. B **103**, 4730 (1999).
[24] Z. Yu, D. Smith, A. Saxena, R. Martin, and A. Bishop, Phys. Rev. Lett. **84**, 721 (2000).
[25] M. A. Palenberg, R. J. Silbey, M. Malagoli, and J. L. Brédas, J. Chem. Phys. **112**, 1541 (2000).
[26] J. V. Selinger and R. F. Brunisma, Phys. Rev. A **43**, 2910 (1991).
[27] A. Troisi, A. Nitzan, and M. A. Ratner, J. Chem. Phys. **119**, 5782 (2003).
[28] W. Pisula, M. Kastler, D. Wasserfallen, M. Mondeshki, J. Piris, I. Schnell, and K. Müllen, Chem. Mater. **18**, 3634 (2006).
[29] A. M. van de Craats, J. M. Warman, A. Fechtenkotter, J. D. Brand, M. A. Harbison, and K. Müllen, Adv. Mater. (Weinheim, Ger.) **11**, 1469 (1999).
[30] R. E. Chandler, A. J. Houtepen, J. Nelson, and D. Vanmaekelbergh, Phys. Rev. B **75**, 085325 (2007).
[31] P. G. Schouten, J. M. Warman, M. P. de Haas, C. F. van Nostrum, G. H. Gelinck, R. J. M. Nolte, M. J. Copyn, J. W. Zwikker, M. K. Engel, M. Hanack, Y. H. Chang, and W. T. Ford, J. Am. Chem. Soc. **116**, 6880 (1994).